High spatial resolution traffic flow and emissions based on taxi GPS data in Bangkok, Thailand

Manlika Sukitpaneenit[1] and Marc E. J. Stettler[1*]

[1] Centre for Transport Studies, Department of Civil and Environmental Engineering, Imperial College London, London SW7 2AZ, United Kingdom

* Corresponding author. E-mail address: m.stettler@imperial.ac.uk

Abstract

High spatial resolution traffic flow is an important input variable for vehicle emissions estimates and health impact assessments. Due to the limited number of fixed detectors on roads, it is a challenging task to estimate the traffic flow on the entire the road network particularly in developing countries. In this study, we demonstrate a methodology for predicting traffic flow using the GPS data from approximately 3,000 taxis to estimate the average vehicle speed on each road link. The fundamental diagram, describing the relationship between traffic flow, speed, and density, is applied to estimate the hourly traffic flow. The methodology is applied to a case study in Bangkok Metropolitan Region (BMR), Thailand. COPERT, an average speed emissions model, is used to calculate the total emissions and spatial distribution of Particulate Matter less than 2.5 microns in diameter ($PM_{2.5}$) and Nitrogen Oxide (NOx) at road links. The results show that the total emissions of $PM_{2.5}$ and NOx were 9.67×10^3 and 329.57×10^3 kg/day respectively. Due to a large number of heavy-duty trucks, highways have the highest $PM_{2.5}$ and NOx emissions.

1. Introduction

Motorised vehicles are an important source of urban air pollution. To improve the accuracy of health impact assessments, vehicle emissions need to be estimated at a high spatial and temporal resolution (Jing *et al.*, 2016). Vehicle emissions are usually estimated by one of two approaches; top-down and bottom-up. The top-down approach is useful when the local detail information is inadequate (Palacios, Martin and Cabal, 2001). This approach estimates vehicle emissions based on statistical data such as the number of vehicle registration, annual or daily travelled distance, and average speed of the entire city. Then, emissions are allocated using a spatial surrogate such as population, road density, and road hierarchy (Cai and Xie, 2007). However, using top-down approach has some limitations; for example, a vehicle can be registered in a certain city but be used in a different city (Coelho *et al.*, 2014). An allocation of vehicle emissions might cause an underestimation or overestimation particularly in the region that has large variations of vehicle activities (Liu *et al.*, 2018). The bottom-up approach relies on using more detailed emission factors that change according to vehicle speed, vehicle technology, operating condition and environment (Pu *et al.*, 2015). The approach also requires comprehensive traffic parameters such as traffic flow, and speed in order to improve the accuracy of emissions estimates. Therefore, this approach generates a high spatial resolution emissions which is an important tool for health impact assessment (Wang *et al.*, 2009).

Several studies have been carried out to estimate vehicle emissions using the bottom-up approach. They obtained link-based traffic parameters (vehicle speed and traffic flow) from traffic simulation models such as VISSIM (Stevanovic *et al.*,2009), PARAMICS (Misra, Roorda and Maclean, 2013), VISUM (Pu *et al.*, 2015), and TransCAD (Zhang *et al.*, 2016). Although the traffic simulation models generate a high temporal-spatial resolution of traffic

parameters, the simulated data diverges from real traffic situations, which could affect the accuracy of vehicle emissions estimates (Liu *et al.*, 2018). For this reason, collecting the real traffic flow and vehicle speed are promising technique for quantifying vehicle emissions.

Conventionally, traffic parameters are obtained by fixed sensors such as loop detectors or cameras (Chiabaut, Buisson and Leclercq, 2009), which provide the traffic volume and occupancy used to calculate flow and density at a specific location (Kawasaki *et al.*, 2018). However, most of the fixed sensors are installed near intersections or on major roads and tend to be limited in spatial coverage. Loop detectors cannot obtain traffic parameters across the road network, which is a significant constraint to the high spatial resolution vehicle emissions estimates.

As an alternative, vehicles fitted with GPS devices, called probe vehicles, are increasingly common and provide the potential to monitor traffic in the areas where fixed sensors are not installed (Nanthawichit, Nakatsuji and Suzuki, 2003). This means that the high spatial resolution traffic data can be acquired over almost the entire the road network (Herrera *et al.*, 2010; Gayah and Dixit, 2013). However, probe vehicle data do not directly provide flow or density information (Neumann *et al.* 2013) and exogenous assumptions are required to estimate traffic flow (Kawasaki *et al.*, 2018).

Although various studies have used probe vehicles to predict traffic information, most of them rely on both data from probe vehicles and additional traffic sensors such as loop detectors or video image processing system. Using a macroscopic traffic flow model, Nanthawichit, Nakatsuji and Suzuki (2003) combined the traffic data from both probe vehicles and loop detectors to estimate traffic states on a road segment of an expressway in Tokyo spanning 5.5km and their results showed that the estimation errors can be reduced by 20-40% for traffic flow estimation and 70-85% for speed and density relative to conventional estimates (i.e. data from loop detectors only). They also recommended that a highly complex simulation model might not be necessary if traffic data covers most parts of the road networks. Guhnemann et al. (2004) used the fundamental diagram between the speed-flow relationship to estimate traffic flow from GPS speed in Berlin, and loop detector data was used to calibrate the proposed model. They found that the speed values estimated by loop detectors were about 50% higher than the probe vehicles speeds as most of the detectors were installed away from intersections. Neumann et al. (2013) also applied the fundamental diagram to estimate traffic flow from probe vehicle data with a wide spatial coverage in Berlin, and Bayesian networks were applied to infer the traffic flow at a given speed range. However, the road classification (i.e. major road, highway) which could affect the traffic flow characteristics was not included in their model. Nagle and Gayah (2013) discussed the use of probe vehicles, which they concluded that the percentage of probe vehicles had to be known in advance, which was not the case in their study or in most other studies. Seo, Kusakabe and Asakura (2015) estimated the flow, density, and speed from the probe vehicle data by employing a spacing measurement equipment. Although they were able to accurately estimate hourly traffic volumes, their method required observed spacings and positions of some of the vehicles in the route. Finally, Ji et al. (2018) used data from both taxi GPS and loop detectors to estimate the traffic density. However, their method required knowledge of the percent of probe vehicles in the traffic stream, which may not always be readily available.

Based on the literature review, it can be seen that probe vehicle data could be a promising source to estimate traffic flow and other traffic parameters such as speed and density. However, we have identified potential limitations from the methodology of previous studies because they tend to depend on the probe penetrate rate, loop detectors or some special types of equipment for flow estimations. Some studies do not include the variation of traffic flow due to different

road types. To overcome the limitations of existing studies, this research therefore aims to: (i) use data from probe vehicles and the fundamental diagram theory to estimate the traffic flow at a high spatial resolution; and (ii) use the estimated of the traffic flow to quantify the emissions attributable to motorised vehicles. The novelty of this research is quantifying the total, spatial and temporal vehicle emissions in BMR for the first time using a high-resolution traffic flow methodology.

The rest of this paper is arranged as follows: Section 2 describes the methodology; Section 3 describes the study area where this methodology is implemented; Section 4 presents the results aligned to the objectives of this paper; and Section 5 summarises and concludes the key findings from this paper.

2. Methodology

2.1 Traffic flow estimations

In this study, the traffic flow for each road link during each hour is calculated using the fundamental diagram. The fundamental diagram represents a steady-state relationship between the traffic flow, average speed, and density as represented in Eq. 1 (Kawasaki *et al.*, 2018),

$$q = \bar{v}k \tag{1}$$

where q is traffic flow (veh/h), k is traffic density (the number of vehicles per road length, in units of veh/km), and $\bar{v}$ is average speed (km/h).

The average speed of traffic is related to the traffic density. Therefore, the traffic density can be estimated from the average speed of probe vehicles on each road link. Two different speed-density relationships were selected and compared, namely the Greenberg (Eq. 2) and Underwood (Eq. 3) models. Figure 1 shows the relationship between $\bar{v}$ and k of Greenberg and Underwood model. Greenberg assumed a logarithmic model which k tends to zero and $\bar{v}$ tends to infinity. Underwood assumed an exponential model which when k is infinity when $\bar{v}$ becomes zero.

Greenberg (1959)
$$\bar{v} = v_c \ln\left(\frac{k_j}{k}\right) \tag{2}$$

Underwood (1961)
$$\bar{v} = v_f \exp\left(-\frac{k}{k_c}\right) \tag{3}$$

where v_f is free-flow speed (km/h), v_c is an optimum speed (km/h), k_c is an optimum density (the traffic density at maximum flow, in units of veh/km, and k_j is traffic jam density (veh/km).
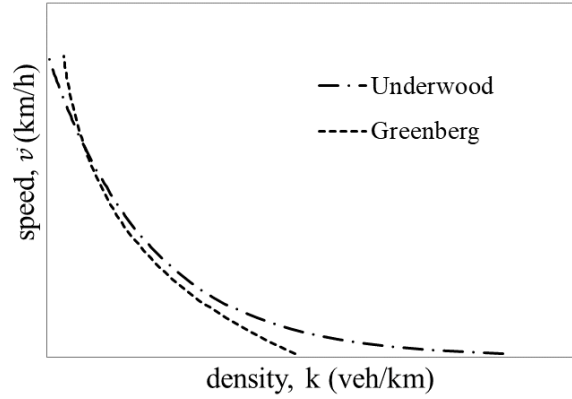
Figure 1. Relation between speed and density

For each road link: (i) $\bar{v}$ is estimated by taking the mean of the instantaneous speed recorded by the probe vehicles; (ii) k is calculated using the $\bar{v} - k$ relationship in Eq. 2 and 3; and (iii) with these k and $\bar{v}$, the speed-flow-density relationship is then used to estimate q. The assumptions for the v_f, v_c, k_j and k_c are presented in Table 1. The v_f refers to the speed limit regulation which is 90, 80, and 60 km/h for highway, arterial and minor roads (Department of Highway, 1992).

A Monte Carlo method is used to quantify the uncertainties in the estimated q: the calculation of q for each road link is repeated 1,000 times using random k_c, k_j and v_f values sampled from probability distributions based on a review of existing literature, which is described in Appendix A. Uncertainty in k_c, k_j was assumed to be represented by a triangular distribution, which is appropriate for situations in which the distributions of variables are not exactly known (Chidsanuphong and Gibson, 2015). The histogram of k_c, k_j is shown in Appendix A. The minimum value was 92 veh/km for k_j and 24 veh/km for k_c; the maximum value was 168 veh/km for k_j and 50 veh/km for k_c; and mode value was 144 veh/km for k_j and 30 veh/km for k_c.

The v_f assumed a normal distribution; the mean was set according to the speed limit regulation and the standard deviation (SD) was ±10 km/h as a 'rule of thumb' to obtain v_f without justification (Deardoff, Wiesner and Fazio, 2011). The 95% confidence intervals (C.I.) for these random parameters are also presented in Table 1. The mean of a 1,000 member ensemble is reported as the estimated traffic flow.

Table 1 Assumptions of input parameters used for Eq. (2) and (3). The v_f was assumed to be a normal distribution; and the k_c and k_j was assumed to be triangular distribution.

Road type	Free-flow speed (v_f km/h) (mean ±SD)	Optimum speed (v_c km/h)	Range of jam density (k_j veh/km)	Range of optimum density (k_c veh/km)
Highway	90 (±10%)			
Arterial	80 (±10%)	32.5[1]	92-168[2]	24-50[2]
Minor	60 (±10%)			

(1) Wathanachingrot and Kasikitwiwat (2014)
(2) References see in Appendix A

To validate our traffic flow estimates, we compare to a set of observations obtained from two sources: (i) the Transport and Planning Department of Bangkok Metropolitan Administration, which provides traffic count data during peak and off-peak hours on arterial roads; and (ii) the Department of Highway, which provided average daily travel (ADT) on highways. In this study, we selected 19 arterial roads (10% of the total length of arterial roads) and 13 highways (11% of the total length of highways) to represent the entire the road network in BMR. There is lack of observations on minor roads.

2.2 Average road speed calculation

To determine the average road speed on each road link i and time t ($\bar{v}_{i,t}$), we matched the locations of probe vehicle data point onto the digital road map by using the 'Snap' function in ArcMap 10.6. Each GPS data point was mapped on to the nearest road edge. A sample of results of the map matching was checked to ensure that the trajectory of individual vehicles was continuous. GPS data not matched to a road within 20 meters were removed. $\bar{v}_{i,t}$ is then calculated as the mean of probe vehicle observations in the time period,

$$\bar{v}_{i,t} = \frac{1}{N_{i,t}} \sum_{j=1}^{N_{i,t}} v_j^{i,t} \tag{4}$$

where $\bar{v}_{i,t}$ is the average speed of link i at time t; $v_j^{i,t}$ is the instantaneous speed of GPS point j on the link i in time t; $N_{i,t}$ is the total number of GPS data points on the link i in time t.

Since the average speeds in this study were computed by using the instantaneous speeds derived from taxi GPS; there may be some sources of error arising from the different behaviour of taxis relative to private vehicles: taxi drivers typically drive more slowly when they are waiting for passengers and drive faster when occupied. Therefore, the estimated speeds were reduced by 15% as recommended by the Office of Transport and Traffic Policy and Planning (OTP, 2010). Finally, the traffic flow was estimated from the average speed based on the fundamental diagram as described in Section 2.1. Note that unlike other studies, this method does not require a-priori knowledge of the proportion of vehicles that are probe vehicles, however it does require us to assume that all types of vehicles have the same average speeds on the same link.

2.3 Vehicle emissions estimates

Emission factors of PM$_{2.5}$ and NOx for each vehicle category under different $\bar{v}_{i,t}$ were calculated based on COPERT V, an average speed emission model used to predict vehicle emissions relies on speed-dependent functions (Sun, Jiang and Gao, 2016). The total vehicle emissions on each road link were calculated using Eq.5:

$$E_{c,i,t}^p = \sum_c EF_{c,i,t}^p \times q_{c,i,t} \times L_i \tag{5}$$

where $E_{c,i,t}^p$ is the emission of pollutant p for vehicle category c on road link i at time t (g/h); $EF_{c,v,t}^p$ is the emission factor of pollutant p for vehicle category c at average speed $\bar{v}$ (g/veh/km) on link i at time t; $q_{c,i,t}$ is traffic flow of vehicle category c on link i at time t (veh/h); L_i is the length of road link i (km).

3. Study area

The methodology described above is applied in the BMR, Thailand. The BMR consists of six provinces including Bangkok, Nonthabutri, Pathum Thani, Samut Prakarn, Samut Sakorn, and

Nakhon Pathom. However, we excluded the Nakhon Pathom province in this study because taxi data was not available. Figure 2a presents the study area and road networks in BMR. The roads in the BMR are separated into three categories: highways, arterial roads, and minor roads. Highways are a road that links Bangkok and the metropolitan area (Cheewaphongphan *et al.*, 2017); arterial roads are main roads where traffic flow can be interrupted by signalized intersections; and minor roads are branches of each arterial road (Srisakda, 2017).

3.1 Probe vehicle data

The probe vehicle data is provided by the Intelligent Traffic Information Center Foundation (ITIC), of which data were collected daily from approximately 3,000 taxis in June 2017. The probe vehicles transmitted data every 60 seconds, and each GPS data point includes the vehicle ID, latitude, longitude, speed, direction, and engine status (on/off). Fig. 2b illustrates an hour spatial distribution of GPS data points on 7 June 2017.
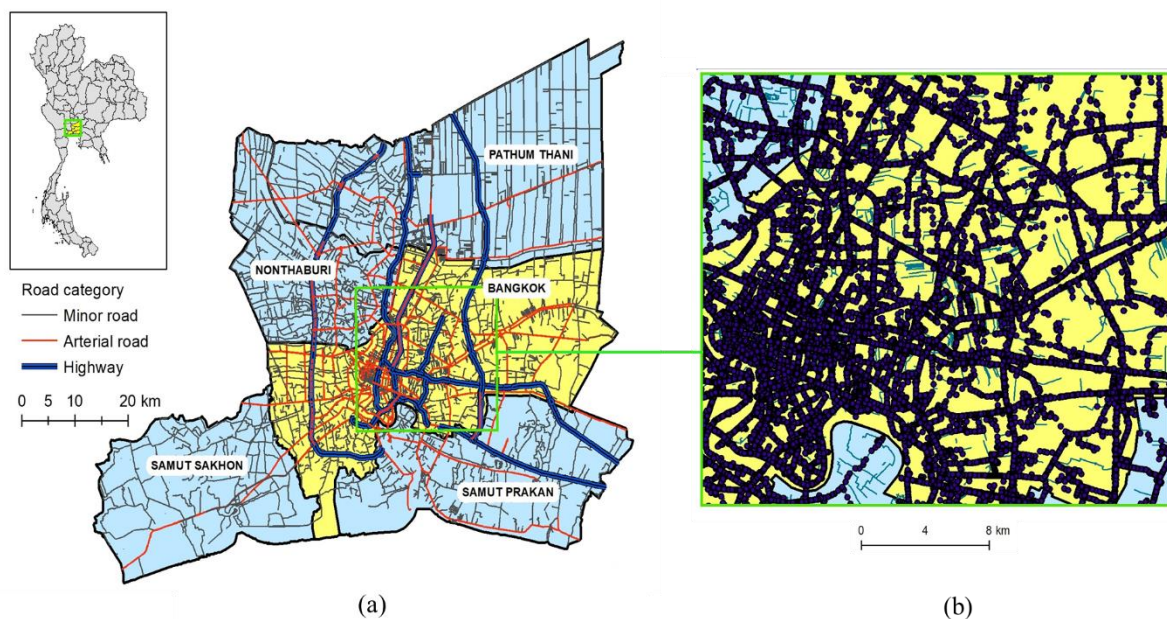

(a)   (b)

Figure 2. Study area (a) road network of Bangkok Metropolitan Region; (b) Spatial distribution of GPS data points on 7 June 2017 during 08.00 - 09.00

3.2 Vehicle fleet composition

Estimates of emissions from motorised vehicles must account for the composition of the fleet. The number of vehicles by types, fuel types, and emission standards in 2017 were obtained from the Department of Land Transport (DLT), the Department of Highway (DOH), and the Department of Transport and Planning-Bangkok Metropolitan Administration. Vehicles in the study were classified into 4 categories: passenger cars (PC), light-duty trucks (LDT), heavy-duty trucks (HDT), and buses. The categories were further divided by types of fuel and Euro emission standards. The data corresponded to vehicle fleet composition on different road types in BMR are presented in Figure 3. We note that motorcycles were not included in the estimates of vehicle emissions because of the lack of data on the traffic flow attributable to motorcycles (MC) and this is a topic for future work.
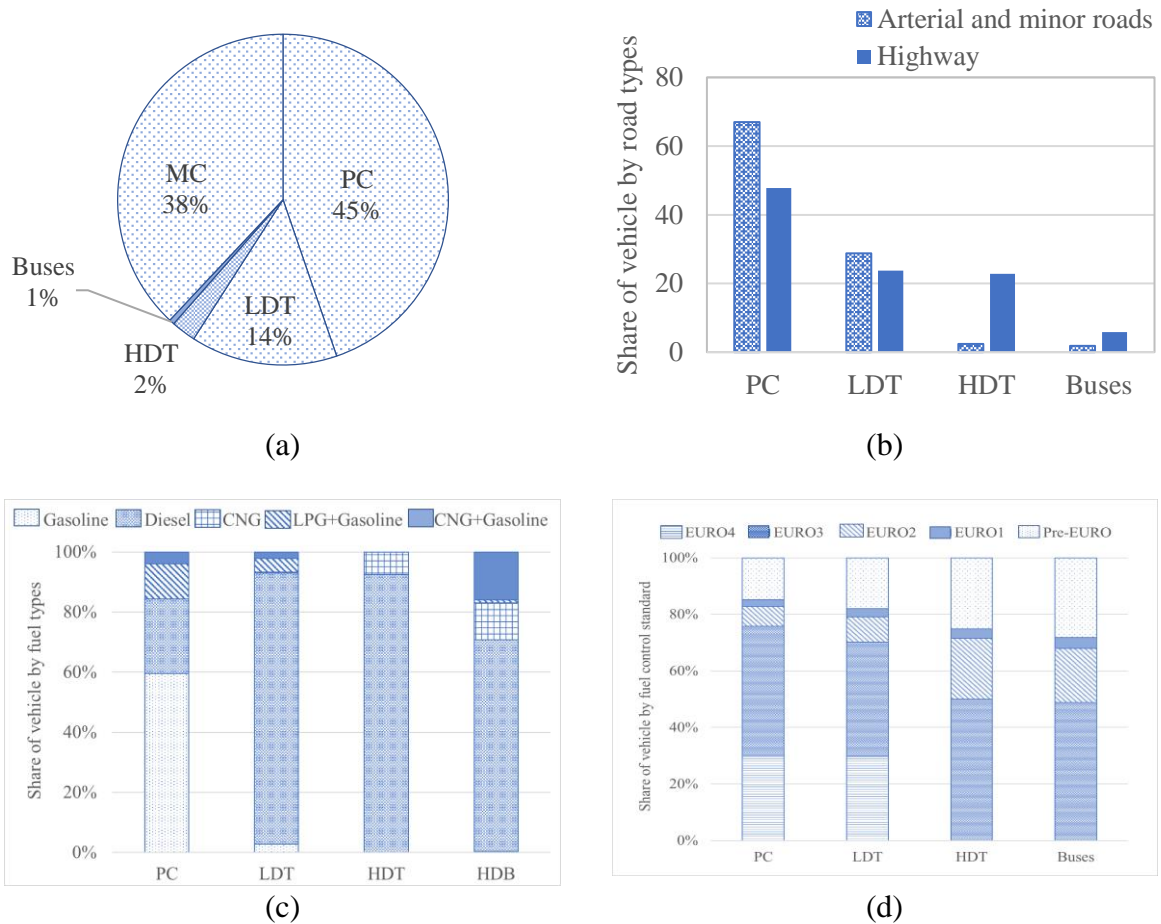
Figure 3. Vehicle fleet composition in BMR in 2017 classified by: (a) vehicle types; (b) road types; (c) by EU emission standard; and (d) by types of fuel used. Remark: PC = passenger cars; LDT = light duty trucks; HDT = heavy duty trucks; MC = motorcycles; CNG = compressed natural gas; and LPG = liquefied petroleum gas. (DLT (2019); DOH (2019))

4. Results and discussion

4.1 Distributions of average speeds in BMR

Figure 4 presents the hourly average speeds of the different road types over 24 hours, and the estimated speeds are divided into 21 bins ranging from 10 – 110 km/h. It should be noted that all speeds below 10 km/h were grouped in speed bin 1 and the speeds over 110 km/h were grouped in speed bin 21. In particular, we observed two types of distributions where the hourly average speeds are: (i) normally distributed, which mostly happened during off-peak hours; and (ii) lognormally distributed with positive skewed (skewed right), mainly during peak hours. Nevertheless, we note that the distribution differs between each road type and the time of day.

For highways, the skewed right distribution mainly occurred in the morning (07:00 to 09:00) and evening peak (17:00 to 19:00), while the normal distributions were observed during the off-peak periods with an average speed of 50 km/hr. For the arterial roads, the normal distribution was observed from 10:00 p.m. until 06:00 a.m., whereas the skewed right distributions were observed during the day. The skewed right distributions on the arterial roads imply that traffic congestion predominantly occurs during the morning and the evening peak.

In the case of minor roads, 80% have a skewed right distribution and with an average speed of about 20 km/h and below. We note that no significant changes to the average speed were observed over time. This may indicate that the vehicles travel slowly due to the limitation of road characteristics (two lanes and narrow width), traffic congestion may not be a major cause of low speed on the arterial and minor roads.
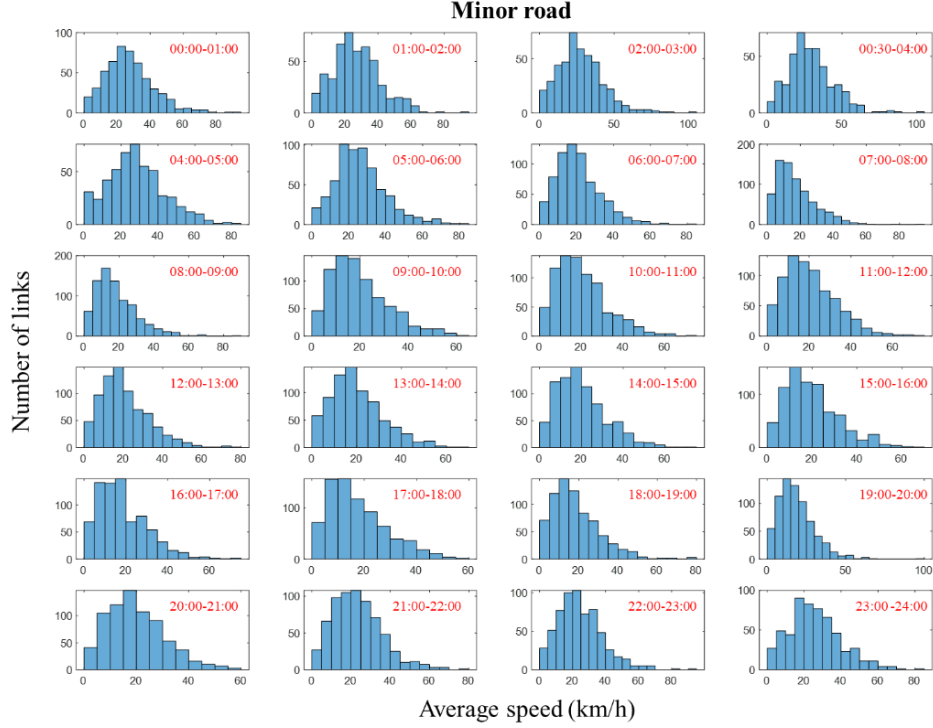

Highway
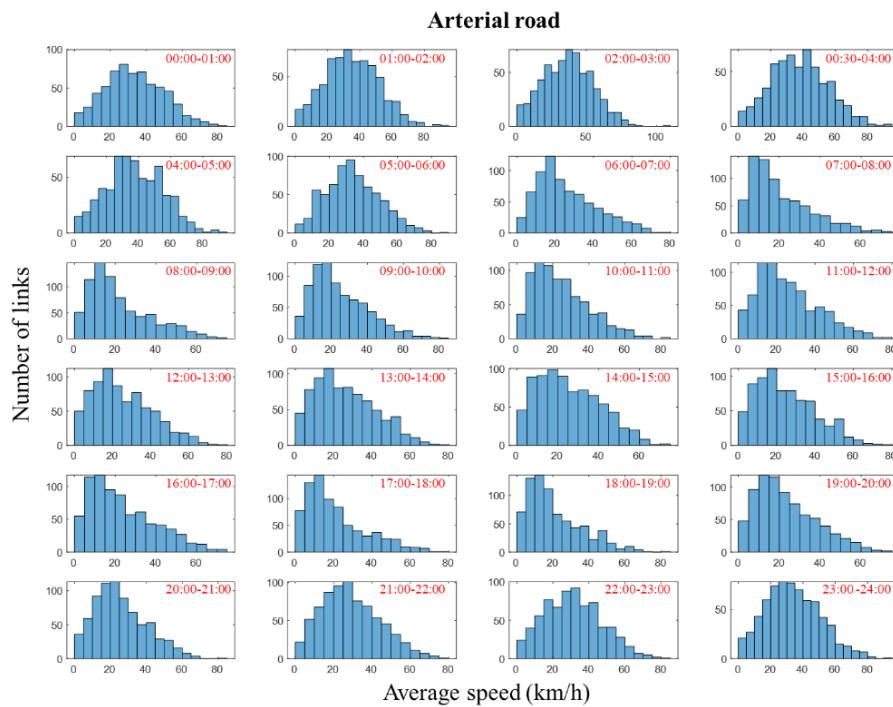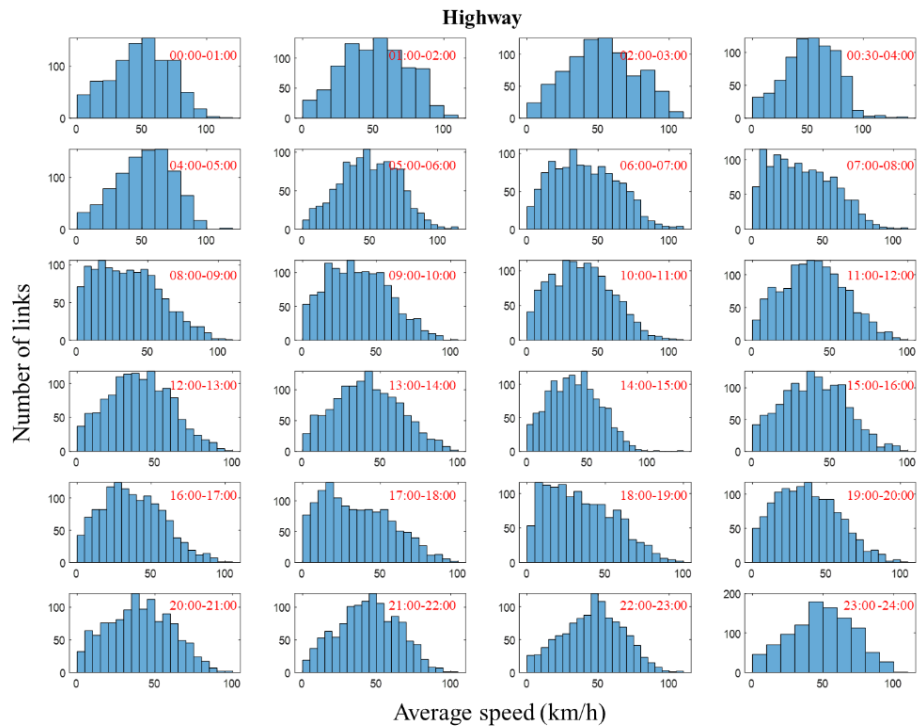
Arterial road

Figure 4. The distributions of the hourly average speed of the: (a) highways; (b) arterial road; and (c) minor road.

4.2 Traffic flow estimations

To validate the estimated q, we used a parity plot to compare the estimated and observed q in the form of the coefficient of determination (R^2) and Normalised Mean Absolute Error (NMAE) as presented in Figure 5. For both highways and arterial roads, the q estimated from the Underwood model (Highways: $R^2 = 0.825$, NMB = -5%; Arterial roads: $R^2 = 0.793$, NMB = -17%) is superior to the Greenberg model (Highways: $R^2 = 0.777$, NMB = -110%; Arterial roads: $R^2 = 0.665$, NMB = 93%). Considering the regression coefficient, Underwood model is close to 1.000 (0.992) on highways and it underestimates the traffic flow on arterial road by 23% (0.774). For Greenberg, it underestimates on highways by -52% (0.484) and overestimates on arterial roads by 120% (1.221).

For both models, we also found that the R^2 values on arterial roads were 5% (by Underwood model) and 14% (by Greenberg model) lower than on highways. This could be due to widespread interruption of the traffic flow by signalised intersections. In theory, the fundamental diagram assumes a steady-state relationship between q, k, and v. However, there are several interventions on arterial roads such as signalised intersections and U-turns, which could affect the estimated q from fundamental diagrams. In addition, the traffic count reported by the Transport and Planning Department of Bangkok Metropolitan Administration was conducted at the intersections which could be affected by the light signals. Based on these validation results, we therefore estimate q from the Underwood model to quantify the emissions from motorised vehicles.
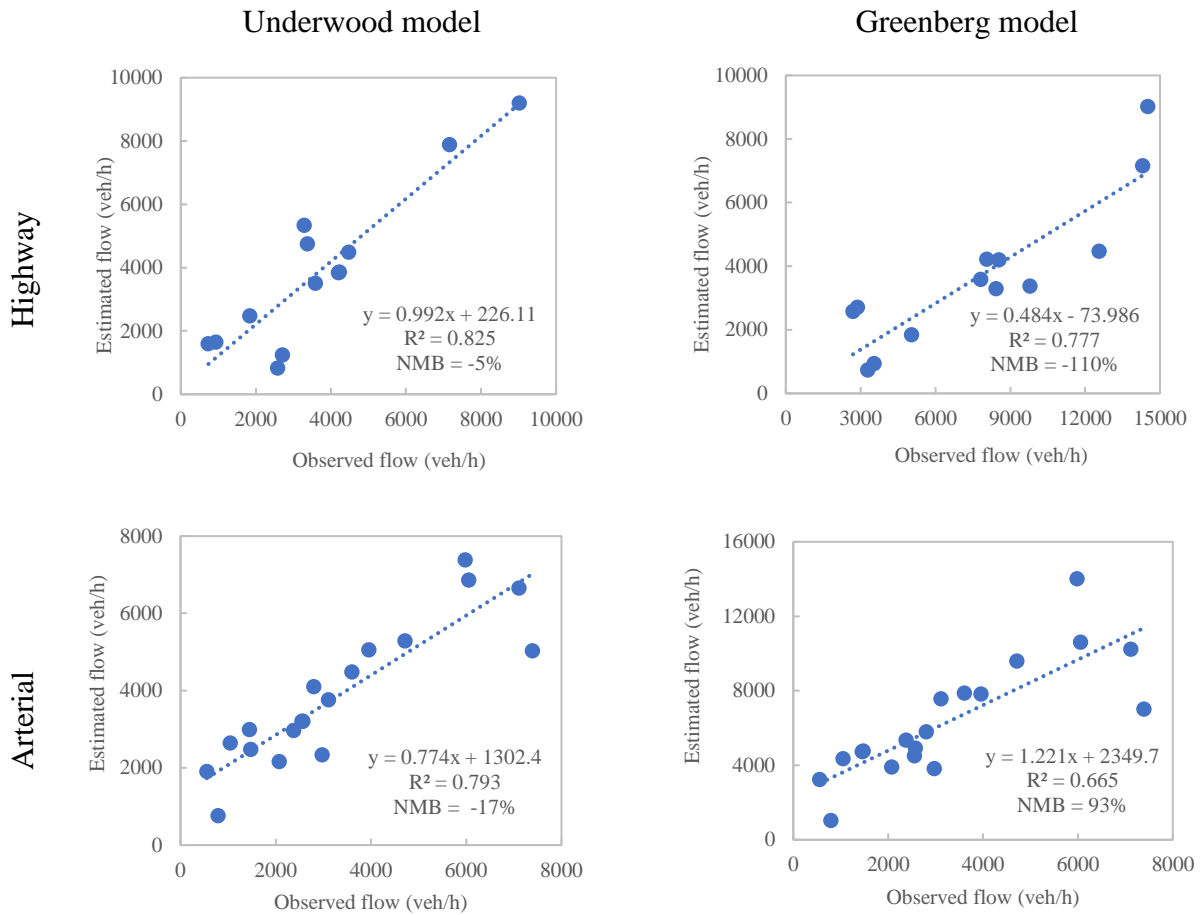
9

Figure 5. Validation of the observed flow against the estimated flow by: (a) Underwood model; and (b) Greenberg model.

4.3 Temporal and spatial distribution of estimated traffic flow

According to the temporal variations of the traffic flow averaged throughout the month (Figure 6), the estimated traffic flow on the highway increases continually from 05:00 a.m. and remains steady throughout the day (at 2200 veh/h) before decreasing to below 2000 veh/h after 23 p.m.. The trend of traffic flow on arterial and minor roads is slightly different from the highway which remains relatively stable at around 1600 and 1300 veh/h during the day respectively.
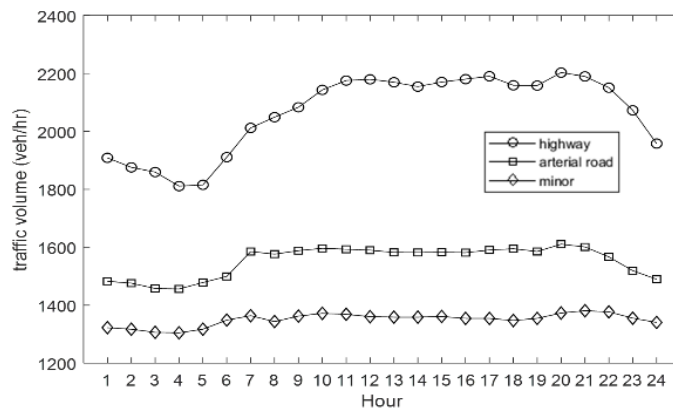

Figure 6. Temporal variations of the estimated traffic flow by Underwood model

10

Figure 7 illustrates the spatial distribution maps of the hourly traffic flow in three periods in BMR. The maps demonstrate that high traffic flow (>3000 veh/h) was observed in the centre of BMR and some roads that link Bangkok to neighbour provinces particularly in the west and southwest of BMR. However, the pattern of spatial distributions did not significantly change according to the time of day.
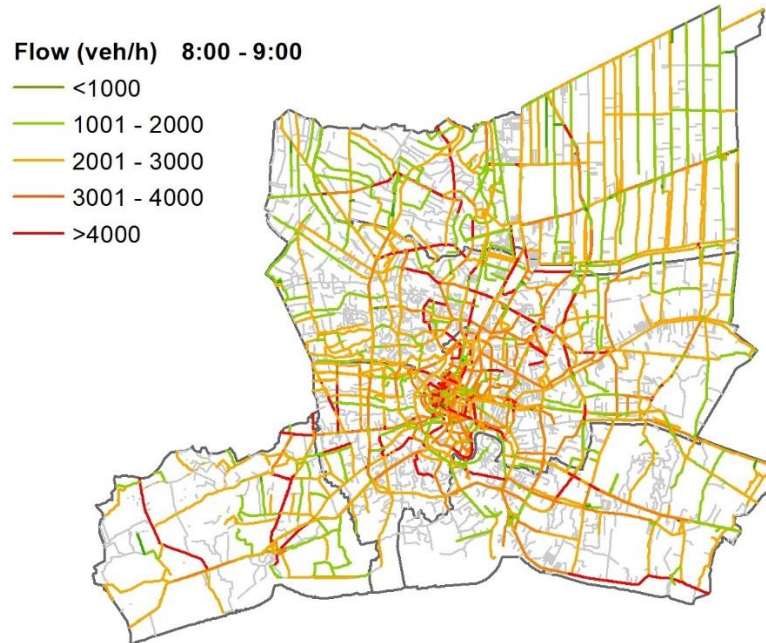
(a)
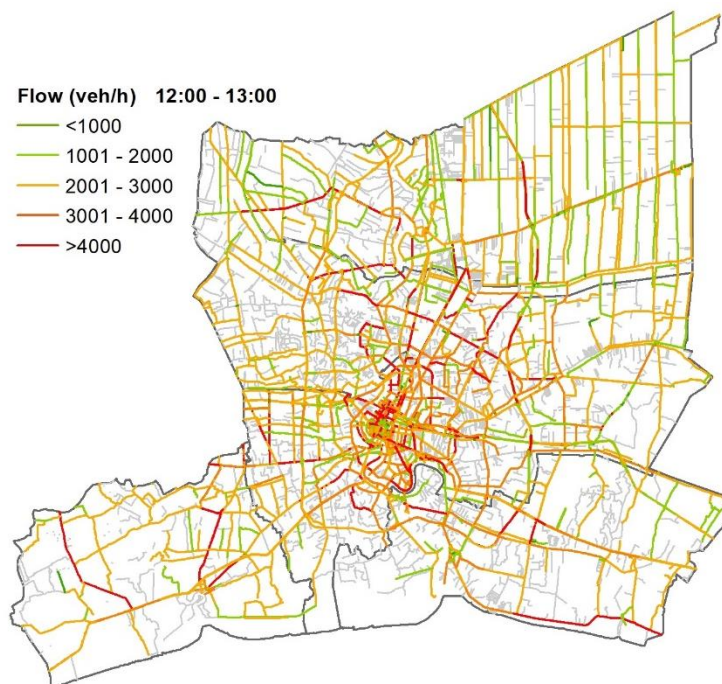
(b)
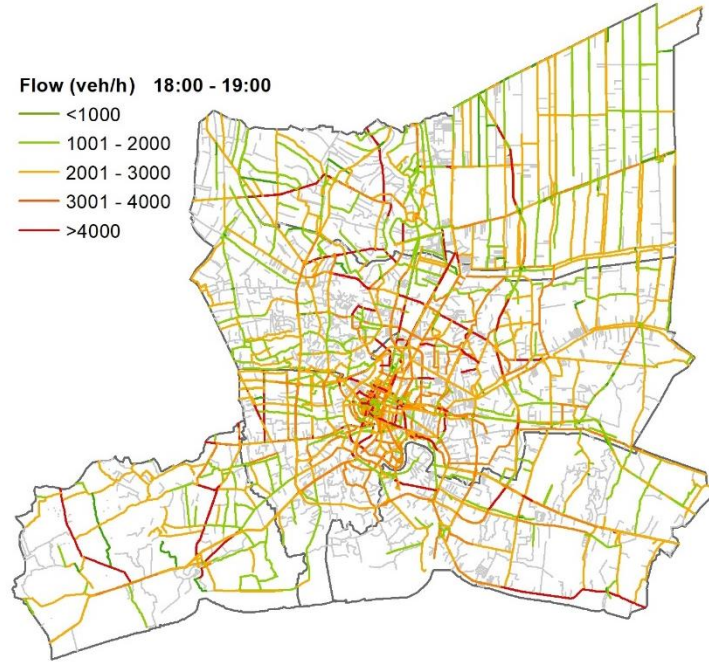
(c)

Figure 7. Spatial distribution of traffic flow during three periods; the morning peak hour (a), off-peak (b), and the evening peak hour (c) in BMR.

4.4 Temporal and spatial variation of vehicle emissions

We compute the vehicle emissions on each road link based on the methodology described in Section 2.3. Due to lack of data on the emission factors for (i) PC with gasoline/CNG (ii) bi-fuel HDT and buses, we used the gasoline and diesel emissions factors instead respectively. The results showed that the total emissions of $PM_{2.5}$ and NOx were 9.67 x10^3 and 329.57 x10^3 kg/day respectively. As summarised in Table 2, the emission allocation patterns by vehicle types show that the HDT was the major contributor of both $PM_{2.5}$ (36% of the total emissions) and NOx (50% of the total emissions) in BMR. Buses ranked second for NOx and the third of $PM_{2.5}$ emissions. Although PC was the largest share of total fleet compositions on all road types, the total $PM_{2.5}$ and NOx emissions were still 56% and 66% lower than heavy duty truck respectively. These results were due to the share of Euro emission standards that almost 50% of cumulative HDT and buses were pre-Euro and Euro 2 emission standard. In contrast, almost 80% of PC were above Euro 2 emissions standard.

Table 2 Daily emissions of different vehicles and road types. Numbers in parentheses indicate the percentage of total fleet emissions.

		$PM_{2.5}$ (×10^3 kg/day)	NOx (×10^3 kg/day)
Vehicle types	Passenger cars	2.14 (16%)	54.90 (17%)
	Light duty trucks	3.74 (29%)	42.12 (13%)
	Heavy duty trucks	4.68 (36%)	164.05 (50%)
	Buses	2.43 (19%)	68.50 (20%)
Road types	Highway	8.07 (62%)	235.12 (71%)
	Arterial	2.47 (19%)	48.18 (15%)
	Minor	2.45 (19%)	46.27 (14%)

Considering the emission allocation patterns by road types, the patterns are similar for both pollutants. Table 2 presents that 62% of PM$_{2.5}$ and 71% of NOx emissions were generated from the highway road network, and 38% of PM$_{2.5}$ and 29% of NOx were from the arterial and minor roads combined. This is because the mode share of HDT and buses on the highway were 7 times higher than on the arterial and minor roads, as seen in Figure 3(a).
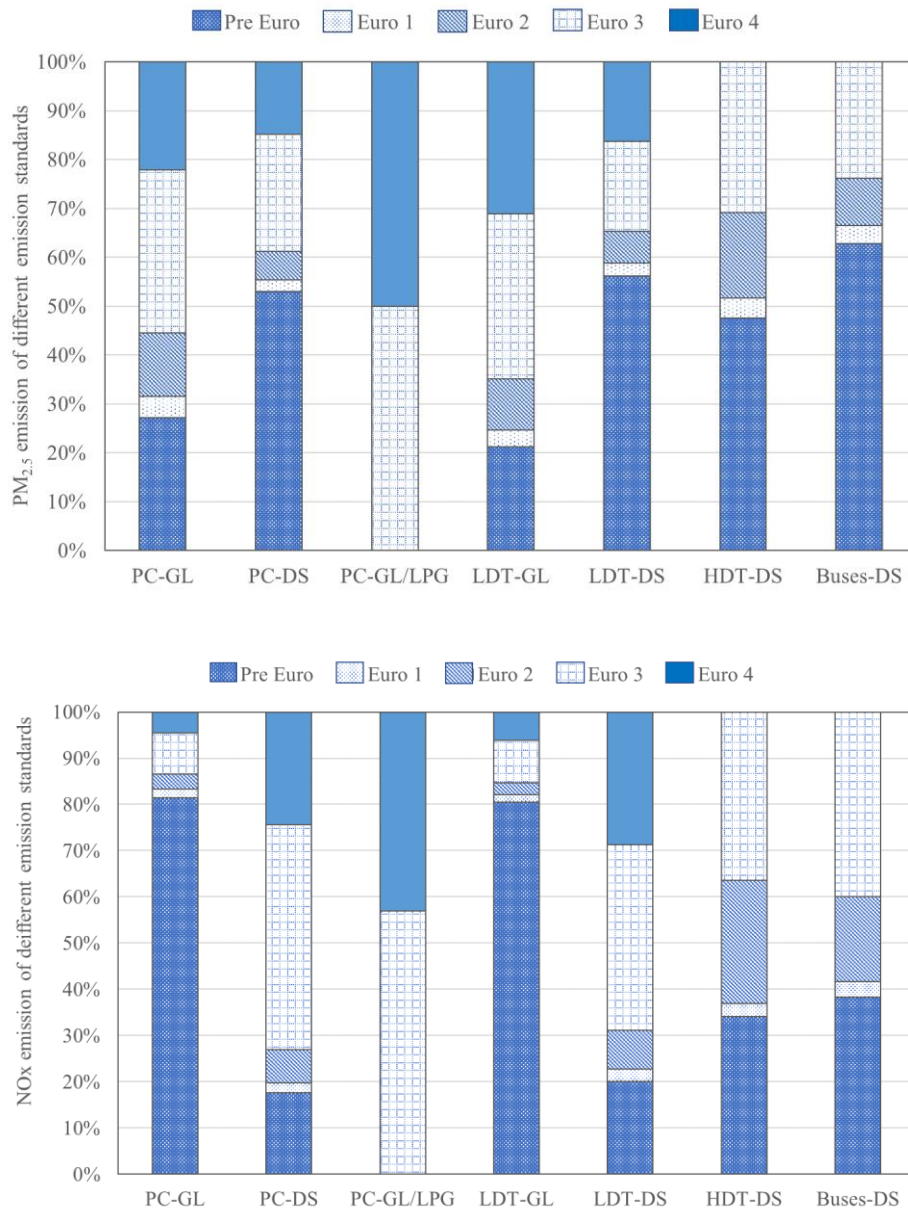

Figure 8. Share of PM$_{2.5}$ and NOx emissions by vehicle-fuel types and emission control standards. Remark: GL= gasoline; DS=diesel; LPG = liquefied petroleum gas.

For the contribution of different fuel types and emission control standards, Figure 8 demonstrates that pre-Euro diesel vehicles were the main contributors of PM$_{2.5}$ (53%), whereas Euro 3 diesel vehicles are the dominant source of NOx (35%). Although NOx emission factors of pre-Euro diesel vehicles are 1.5-2.0 times higher than Euro 3 diesel vehicles, the highest number of Euro 3 diesel vehicles in the traffic flow (48%) contributed to 35% of the NOx emission in BMR.

Figure 9 demonstrates the spatial variation of the hourly average $PM_{2.5}$ and NOx emission in three periods: (i) 08:00 to 09:00; (ii) 12:00 to13:00; and (iii) 18:00 to 19:00. It can be seen that $PM_{2.5}$ and NOx emissions show similar trends throughout the day, where they remain constant emissions over the different periods. In addition, the spatial distribution of the emissions has a good agreement with the traffic flow distributions as presented in Figure 7. Both PM and NOx emissions are mainly concentrated in the centre of Bangkok (with a high traffic volume and low average speed) and decreases from the centre to the periphery of BMR. Although the highest traffic congestion was found in the centre of BMR, the highest $PM_{2.5}$ and NOx emissions were mostly found on the highways at the boundary between Bangkok and the neighbours, particularly in the western part of BMR. The main reason for the high emissions is the high volume (approximately 20% of total fleet) of HDT crossing from the south to the north of Thailand.
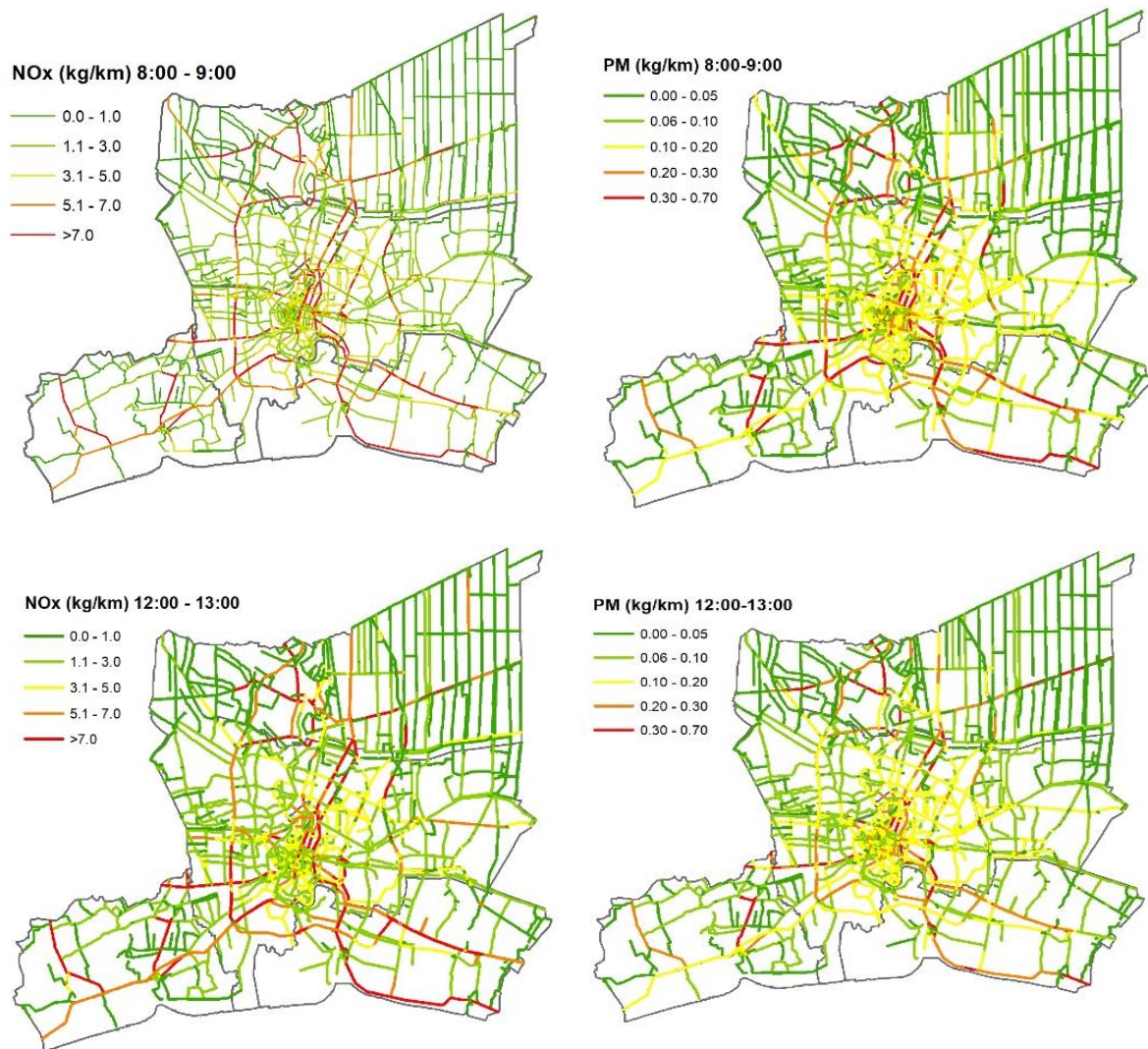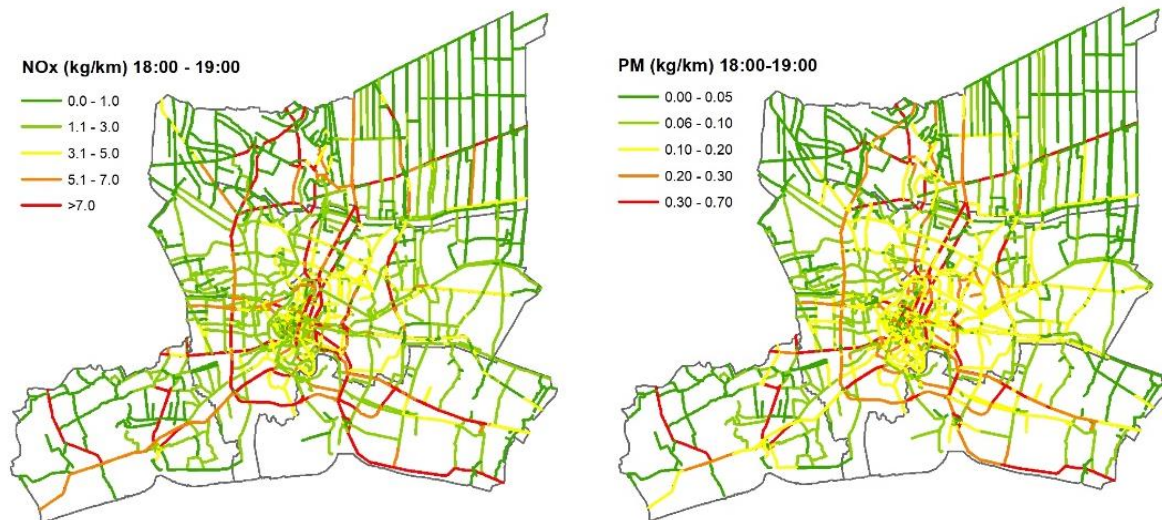
Figure 9. Spatial distribution of the hourly $PM_{2.5}$ and NOx in BMR during three periods: (i) 08:00 to 09:00; (ii) 12:00 to13:00; and (iii) 18:00 to 19:00.

4.5 Comparison with other studies

The vehicle emissions of $PM_{2.5}$ and NOx are compared with Cheewaphongphan *et al.*(2017) which is the most recent study that measured these emissions in Bangkok. Using a top-down approach, Cheewaphongphan *et al.*(2017) estimated vehicle emission in BMR between 2007 and 2015 with the Greenhouse Gas and Air Pollution Interactions and Synergies (GAINS) model. Two input parameters were used in this study to represent traffic activities: (i) annual distance travelled in BMR; and the (ii) fuel consumptions by vehicle and fuel types which were downscaled from the national data. Since Cheewaphongphan *et al.*(2017) reported the average annual emissions of $PM_{2.5}$ and NOx, while this study reports the emissions per day. We divided their annual emissions with 365 days in order to get the daily emissions. It is an approximation and does not capture the potential day-to-day variation in the emissions.

We note that both the NOx and $PM_{2.5}$ emissions estimated in this study are 4% and 77% lower than Cheewaphongphan *et al.*(2017). The large difference in $PM_{2.5}$ emissions is likely due to three main reasons: (i) our study does not account for motorcycles, which have a significant share in BMR (38% of the total fleet); (ii) the exclusion of the Nakhon Pathom province in this study due to the lack of traffic flow data, which could lead to lower emissions of $PM_{2.5}$ and NOx; and (iii) Cheewaphongphan *et al.*(2017) used $PM_{2.5}$ emissions factors solely on vehicle - fuel types and emission standard, whereas we use emissions factors related to an average speed.

Taking into consideration the share of emissions by vehicle types, they are consistent with the emission contributors. Both studies reported that HDT was a major emitter of NOx (50% in this study and 53% in Cheewaphongphan *et al.*(2017), buses and PC were the second and the third emitters. Considering $PM_{2.5}$, HDT was reported as the main contributor in both studies (36% in this study and 48% in Cheewaphongphan *et al.*(2017); followed by LDT and buses respectively.

Emissions of PM and NOx observed in this study raises important concerns of the strict enforcement of vehicle emission standards particularly for HDT and buses. As seen from the share of vehicle types by Euro standards, almost 50% of HDT and buses were under Euro 2 engines. The phrase-out of low emission control HDT and buses from the road network in

BMR should be the priority of policies addressing air pollution. In addition, Thailand has been complying with Euro 3 for HDT since 2007, the Euro 4 or higher should be enforced as soon as possible to reduce vehicle emissions.

5 Conclusion

High spatial resolution traffic flow and emissions are required to manage the air quality and to assess the health impacts, particularly in the developing countries where vehicle use is increasing. This study quantifies traffic flow and vehicle emissions at a high spatial and temporal resolution across BMR.

Our findings demonstrate that the application of the fundamental diagram could overcome the limitations of existing studies to estimate the traffic flow on each road link. Highway carries the highest traffic flow and has a larger temporal variation (2000 ± 200 veh/h) than arterial and minor roads (1480 ± 50 veh/h and 1300 ± 20 veh/h). The correlation between the observed flow and estimated flow on the highway ($R^2 = 0.825$) is greater than on the arterial roads ($R^2 = 0.793$). The spatial distributions of traffic flow and emissions can help identify the relationship between flow and emissions. 81% and 86% of $PM_{2.5}$ and NOx emissions were mostly found on the arterial roads in the centre of BMR and on highways that connect between BMR and other parts of Thailand. Despite HDT and buses consist of only 4% and 1% of the overall fleet, they emitted 55% and 70% of the total $PM_{2.5}$ and NOx emissions. Therefore, to further control emissions and improve air quality, we recommend more stringent regulations and vehicle standard for HDT and buses.

The validation of estimated emissions with another study found that there are various factors, such as the traffic activity data, emissions factors and methodology, that could contribute to the difference in emissions estimates. Although there is an agreement of NOx emissions between this study and the another (4%), a large significant difference of $PM_{2.5}$ emissions (77%) is presented. The establishment of high spatial resolution of vehicle emissions using our bottom-up approach can better depict vehicle emissions and provide insight to policy.

Finally, we identify several avenues for further research: (i) the relationship between speed and flow could be temporally separated (day and night time) for more accurate traffic flow estimates; (ii) given that the emission factors used in this paper are mainly generated from European fleets, the emissions factor should account for local degradation factors (such as vehicle age, mileage and local environmental conditions) to improve the accuracy of the vehicle emission estimates; and (iii) the uncertainties of the estimated traffic flow should be taken into consideration when estimating vehicle emissions.

References

Aerde, M. Van and Rakha, H. (1995) 'Multivariate calibration of single regime speed-flow-density relationships', in *Proceedings of the 6th 1995 Vehicle Navigation and Information Systems Conference*, pp. 334–341. doi: 10.1109/VNIS.1995.518858.

Cai, H. and Xie, S. D. (2007) 'Estimation of vehicular emission inventories in China from 1980 to 2005', *Atmospheric Environment*, 41(39), pp. 8963–8979. doi:

10.1016/j.atmosenv.2007.08.019.

Cheewaphongphan, P. *et al.* (2017) 'Emission inventory of on-road transport in bangkok metropolitan region (BMR) development during 2007 to 2015 dusing the GAINS model', *Atmosphere*, 8(167). doi: 10.3390/atmos8090167.

Cheng, X., Zhao-wei, Q. and Xiao-ming, C. (2014) 'Analysis of traffic flow speed-density relation model characteristics', *Journal of Highway and Transportation Research and Development*, 8(4), pp. 104–110. doi: 10.1061/JHTRCQ.0000418.

Chiabaut, N., Buisson, C. and Leclercq, L. (2009) 'Fundamental diagram estimation through passing rate measurements in congestion', *IEEE Transactions on Intelligent Transportation Systems*, 10(2), pp. 355–359. doi: 10.1109/TITS.2009.2018963.

Chidsanuphong, C. and Gibson, J. M. (2015) 'Health impact assessment of traffic-related air pollution at the urban project scale: Influence of variability and uncertainty', *Science of the Total Environment*, 506–507, pp. 409–421. doi: 10.1016/j.scitotenv.2014.11.020.

Coelho, M. C. *et al.* (2014) 'Assessment of potential improvements on regional air quality modelling related with implementation of a detailed methodology for traffic emission estimation', *Science of the Total Environment*, 470–471, pp. 127–137. doi: 10.1016/j.scitotenv.2013.09.042.

Deardoff, M. D., Wiesner, B. N. and Fazio, J. (2011) 'Estimating free-flow speed from posted speed limit signs', *Procedia - Social and Behavioral Sciences*, 16, pp. 306–316. doi: 10.1016/j.sbspro.2011.04.452.

Department of Highway (1992) *Highway Act 1992 (in Thai language)*. Available at: http://www.fio.co.th/south/law/8/83.pdf.

Dervisoglu, G., Gomes, G. and Horowitz, R. (2009) 'Automatic calibration of the fundamental diagram and empirical observations on capacity', *Transportation Research Board*, 88(January), pp. 1–14. Available at: http://gateway.path.berkeley.edu/topl/papers/2009TRB_DervisogluEtAll__AutomaticCalibration.pdf.

DLT(Department of Land Trasport) (2019) *Statistics*. Available at: https://web.dlt.go.th/statistics/ (Accessed: 10 May 2019).
DOH (Department of Highways) (2019) *Statistics*. Available at: https://bhs.doh.go.th/en/download/report (Accessed: 11 May 2019).

Easa, S. M. and May, A. D. (1980) 'Generalized procedure for estimating single and two-regime traffic flow models.', *Transportation Research Record*, (772), pp. 24–37.
Erlingsson, S., Jonsdottir, A. M. and Thorsteinsson, T. (2006) 'Traffic Stream Modelling of Road Facilities', in *Transport Research Arena Europe*.

Gayah, V. and Dixit, V. (2013) 'Using mobile probe data and the macroscopic fundamental diagram to estimate network densities', *Transportation Research Record: Journal of the Transportation Research Board*, 2390, pp. 76–86. doi: 10.3141/2390-09.

Guhnemann, A. *et al.* (2004) 'Monitoring traffic and emissions by floating car data', in *ITS-WP-04-07 Monitoring*, p. 19. doi: 10.1002/pola.

Herrera, J. C. *et al.* (2010) 'Evaluation of traffic data obtained via GPS-enabled mobile phones: The Mobile Century field experiment', *Transportation Research Part C: Emerging Technologies*. doi: 10.1016/j.trc.2009.10.006.

Ji, Y. *et al.* (2018) 'Determining the macroscopic fundamental diagram from mixed and partial traffic data', *Promet - Traffic - Traffico*. doi: 10.7307/ptt.v30i3.2406.

Jing, B. *et al.* (2016) 'Development of a vehicle emission inventory with high temporal-spatial resolution based on NRT traffic data and its impact on air pollution in Beijing-Part 1: Development and evaluation of vehicle emission inventory', *Atmos. Chem. Phys*, 16, pp. 3161–3170. doi: 10.5194/acp-16-3161-2016.

Kawasaki, Y. *et al.* (2018) 'Fundamental diagram estimation using GPS trajectories of probe vehicles', *IEEE Conference on Intelligent Transportation Systems, Proceedings, ITSC*, 2018-March, pp. 1–6. doi: 10.1109/ITSC.2017.8317661.

Knoop, V. L. and Daamen, W. (2017) 'Automatic fitting procedure for the fundamental diagram', *Transportmetrica B*, 5(2), pp. 133–148. doi: 10.1080/21680566.2016.1256239.
Kockelman, K. (1998) 'Changes in flow-density relationship due to environmental, vehicle, and driver characteristics', *Transportation Research Record: Journal of the Transportation Research Board*, 1644(2), pp. 47–56. doi: 10.3141/1644-06.

Liu, Y. H. *et al.* (2018) 'A high temporal-spatial vehicle emission inventory based on detailed hourly traffic data in a medium-sized city of China', *Environmental Pollution*, 236, pp. 324–333. doi: 10.1016/j.envpol.2018.01.068.

Lu, Z. and Meng, Q. (2013) 'Analysis of traffic speed-density regression models -A case study of two roadway traffic flows in China', *Civil and Environmental Engineering*, 9(1986), pp. 1–14.

Lum, K. M. and Olszewski, P. S. (1998) 'Speed-flow modeling of arterial roads in singapore', *Article in Journal of Transportation Engineering*, 3(May). doi: 10.1061/(ASCE)0733-947X(1998)124:3(213).

May, A. D. (1990) *Traffic Flow Fundamentals*. New Jersey: Prentice-Hall.
Mazloumian, A., Geroliminis, N. and Helbing, D. (2010) 'The spatial variability of vehicle densities as determinant of urban network capacity', *Philosophical Transactions of the Royal Society A: Mathematical, Physical and Engineering Sciences*, 368(1928), pp. 4627–4647. doi: 10.1098/rsta.2010.0099.

Misra, A., Roorda, M. J. and Maclean, H. L. (2013) 'An integrated modelling approach to estimate urban traf fi c emissions', *Atmospheric Environment*. Elsevier Ltd, 73, pp. 81–91. doi: 10.1016/j.atmosenv.2013.03.013.

Nagle, A. S. and Gayah, V. V. (2013) 'A method to estimate the macroscopic fundamental diagram using limited mobile probe data', in *IEEE Conference on Intelligent Transportation Systems, Proceedings, ITSC*. doi: 10.1109/ITSC.2013.6728521.

Nanthawichit, C., Nakatsuji, T. and Suzuki, H. (2003) 'Application of probe-vehicle data for real-time traffic-state estimation and short-term travel-time prediction on a freeway', *Transportation Research Record: Journal of the Transportation Research Board*, pp. 49–59. doi: 10.1016/j.jneuroim.2017.09.006.

Neumann, T., Bohnke, P. L. and Touko Tcheumadjeu, L. C. (2013) 'Dynamic representation of the fundamental diagram via Bayesian networks for estimating traffic flows from probe vehicle data', *IEEE Conference on Intelligent Transportation Systems, Proceedings, ITSC*, (Itsc), pp. 1870–1875. doi: 10.1109/ITSC.2013.6728501.

OTP, (Office of Transport and Traffic Policy and Planning) (2010) *Development of the ITS Data Integration Center, OTP : Phase II*. Available at: http://www.otp.go.th/uploads/tiny_uploads/ProjectOTP/2552/Project3/1-FinalReport.pdf.

Palacios, M., Martin, F. and Cabal, H. (2001) 'Methodologies for estimating disaggregated anthropogenic emissions — Application to a coastal mediterranean region of Spain', *Journal of the Air & Waste Management Association*, (51), p. 642:657. doi: 10.1080/10473289.2001.10464305.

Pu, Y. *et al.* (2015) 'Impact of license plate restriction policy on emission reduction in Hangzhou using a bottom-up approach', *Transportation Research Part D: Transport and Environment*. Elsevier Ltd, 34, pp. 281–292. doi: 10.1016/j.trd.2014.11.007.

Seo, T., Kusakabe, T. and Asakura, Y. (2015) 'Estimation of flow and density using probe vehicles with spacing measurement equipment', *Transportation Research Part C: Emerging Technologies*. doi: 10.1016/j.trc.2015.01.033.

El Sherief, M. M., Ramadan, I. M. I. and Ibrahim, A. M. (2016) 'Development of traffic stream characteristics models for intercity roads in Egypt', *Alexandria Engineering Journal*. Faculty of Engineering, Alexandria University, 55(3), pp. 2765–2770. doi: 10.1016/j.aej.2016.04.031.

Smirnova, M. N. *et al.* (2016) 'Traffic flow sensitivity to visco-elasticity', *Theoretical and Applied Mechanics Letters*. Elsevier Ltd, 6(4), pp. 182–185. doi: 10.1016/j.taml.2016.05.003.

Soriguera, F. *et al.* (2017) 'Effects of low speed limits on freeway traffic flow', *Transportation Research Part C: Emerging Technologies*, pp. 257–274. doi: 10.1016/j.trc.2017.01.024.

Srisakda, N. (2017) *Development of Method to Estimate Fuel Consumption Reduction Based on Time Sharing of Driving Modes-Case of Promotion of Hybrid Cars in Bangkok*. Nihon University.

Stevanovic, A. *et al.* (2009) 'Optimizing traffic control to reduce fuel consumption and vehicular emissions', *Transportation Research Record: Journal of the Transportation Research Board*, 2128, pp. 105–113. doi: 10.3141/2128-11.

Sun, S., Jiang, W. and Gao, W. (2016) 'Vehicle emission trends and spatial distribution in Shandong province, China, from 2000 to 2014', *Atmospheric Environment*. Elsevier Ltd,

147(X), pp. 190–199. doi: 10.1016/j.atmosenv.2016.09.065.

Wang, H. *et al.* (2009) 'A bottom-up methodology to estimate vehicle emissions for the Beijing urban area', *Science of the Total Environment*. Elsevier B.V., 407(6), pp. 1947–1953. doi: 10.1016/j.scitotenv.2008.11.008.

Wathanachingrot, W. and Kasikitwiwat, P. (2014) 'A study of relationship between traffic flow variables of a roadway in urban area', *UBU Engineering Journal*, 7(1), pp. 37–45. Wu, N. (2002) 'A new approach for modeling of Fundamental Diagrams', *Transportation Research Part A*, 36, pp. 867–884.

Zhang, S. *et al.* (2016) 'High-resolution simulation of link-level vehicle emissions and concentrations for air pollutants in a traffic-populated eastern Asian city', *Atmospheric Chemistry and Physics*, 16(15), pp. 9965–9981. doi: 10.5194/acp-16-9965-2016.

Zhao, N. *et al.* (2009) 'Analysis of traffic flow characteristics on ring road expressways in Beijing', *Transportation Research Record: Journal of the Transportation Research Board*, 2124, pp. 178–185. doi: 10.3141/2124-17.

Appendix A

Eq. (2) and (3) require two input traffic parameters including jam density (k_j) and optimum density (k_c). This study reviewed the values of required parameters from several empirical studies, as presented in Table 3. The distribution of k_j and k_c is presented in Figure A1.

Table A1 Empirical k_j *and* k_c values from literature review

| References	City, period	(k_j, veh/km)	(k_c, veh/km)
May (1990)	Freeway	121	-
Aerde and Rakha (1995)	Amsterdam	115	26
Wu (2002)	Germany, 20 mins	155	30
Smirnova *et al.* (2016)	Beijing, -	150	-
Dervisoglu, Gomes and Horowitz (2009)	California, 92 days	144	20
Erlingsson, Jonsdottir and Thorsteinsson (2006)	Iceland, 5 mins	110	24
Chiabaut, Buisson and Leclercq (2009)	California, 45 mins	130	-
Zhao *et al.* (2009)	Beijing, 24 hrs	140	-
Lu and Meng (2013)	Beijing, 2 mins	114	29
Kockelman (1998)	California, 2 weekdays	125	28
Ni, D. (2016)	-	167	-
El Sherief, Ramadan and Ibrahim (2016)	Cairo, 4 weekdays	168	-
Soriguera *et al.* (2017)	Barcelona, 3 hours	140	30
Knoop and Daamen (2017)	Netherlands, -	144	-
Cheng, Zhao-wei and Xiao-ming (2014)	Beijing, 4 hours	165	-
Lum and Olszewski, (1998)	Singapore, 15 mins	-	58
(Mazloumian, Geroliminis and Helbing, 2010)	-	-	40
(Easa and May, 1980)	-	-	43 & 50
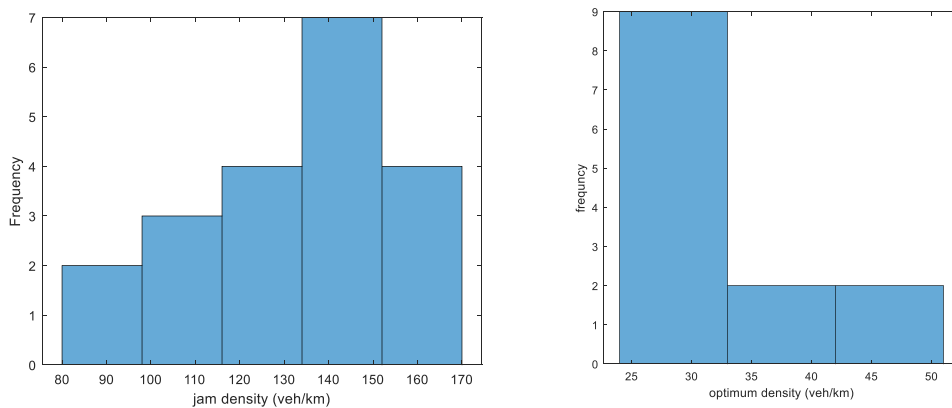
Figure A1 Histogram of jam density (k_j) and optimum density (k_c) from the empirical studies

21